Moment T-matrix approach to e^+-H scattering. I. Angular distribution and total cross section for energies below the pickup threshold

Jeremy R. Winick* and William P. Reinhardt

Department of Chemistry, University of Colorado, and Joint Institute for Laboratory Astrophysics, University of Colorado and National Bureau of Standards, Boulder, Colorado 80309

(Received 27 March 1978)

A formalism is developed for calculation of electron and positron scattering from atoms at low and intermediate energies in terms of appropriate matrix elements of the off-shell T operator. The technique is based on an L^2 discretization of the full electronic Hamiltonian, initially avoiding all specification of channels and asymptotic boundary conditions. Scattering information relating to specific initial and final channels is obtained by taking appropriate off-shell matrix elements, followed by construction of the total real axis discontinuity of the off-shell elements via moment techniques. The formalism is applied to the problem of purely elastic e^+-H scattering, resulting in converged total cross sections and angular distributions below the pickup threshold.

I. INTRODUCTION

The theory of positron-hydrogen scattering has been studied for many years. Massey and Mohr[1] first emphasized the importance of positron interactions in gases and applied various approximations of collision theory to the simplest case of positron–hydrogen-atom scattering. Since nonrelativistic positron-hydrogen scattering is essentially a two-body problem, it would seem reasonable that with the use of computers the problem should now be completely solved. However, accurate results have been obtained only for e^+-H elastic phase shifts for a few partial waves and for the s-wave elastic amplitude up to 30 eV. It is the purpose of this paper to develop a computational formalism suitable for calculation of partial-wave-scattering amplitudes at low and intermediate energies; that is, over the purely elastic region, and at energies above the impact-ionization threshold, where elastic and inelastic positron scattering, positronium pick-up, as well as impact ionization can occur. In the present paper we develop the necessary formalism for such calculations, and apply it to calculate accurate differential and total cross sections in the energy region below the first inelastic threshold, the pick-up threshold at a positron energy of 0.25 a.u. (~6.8 eV). The following paper (Ref. 2) extends the results into the intermediate-energy regime where there is a continuum of open channels. Finding a workable formalism for use in the intermediate-energy region proved to be quite difficult, as is thoroughly documented in Ref. 3. Thus, while methods such as the use of optical potentials,[4] close coupling,[5] adiabatic approximations and polarized orbitals,[6] single-channel variational methods,[7] T-matrix continuation,[8] Fredholm analytic continuation,[9] and T-matrix extrapolation[10] are all viable candidates for calculations of elastic phase shifts, none of these proved suitable for calculations in the intermediate-energy region, below energies where the Glauber,[11] or Born[12] cross sections might be expected to be reliable. The failure[3] of methods (such as those of Refs. 8-10) which might be expected to be effective above the impact-ionization threshold led to development of a moment T-matrix method which combines the basic ideas of Refs. 8–10 in that the detailed specification of boundary conditions is avoided through use of L^2 expansion functions and a subsequent discretization of the full Green's operator $(z-H)^{-1}$, but uses moment techniques,[13,14] rather than analytic continuation[8,9] or extrapolation,[10] to extract the required amplitudes.

Rather than reviewing the standard techniques for calculation of e^+-H elastic phase shifts, a notoriously difficult computational problem, we refer the reader to Refs. 4–10 and to reviews.[15]

The plan of the paper is as follows: In Sec. II we review the T-matrix methods of Schlessinger and Schwartz[8] and Doolen *et al.*,[10] and, in particular, present new numerical results illustrating the difficulties of the T-matrix extrapolation method. In Sec. III we present an extension of the T-matrix techniques introducing the use of moments to extract $\mathrm{Im}[T(E+i\epsilon)]$ followed by calculation of $\mathrm{Re}[T(E+i\epsilon)]$ by a dispersion technique. The Stieltjes method developed by Langhoff and coworkers[14] for extracting continuum information from a finite set of moments is discussed, as is the derivative rule (see Appendix A) method of Heller[16] and Broad.[17] A peculiarity of the e^+-H problem is that the Stieltjes method is unsuitable for numerical work, as is discussed in Sec. IV, where numerical results for purely elastic e^+-H

scattering at energies below the pick-up threshold are presented. Finally, a brief summary is given in Sec. V.

II. T-MATRIX METHODS

The elastic-scattering amplitude $f(k)$ may be determined as

$$f(k) = -(2\pi)T_k(E+i\epsilon)\big|_{E=k^2/2}, \tag{2.1}$$

where $T_k(E+i\epsilon)$ is the elastic, diagonal, off-shell matrix element[18]

$$T_k(E+i\epsilon) = \lim_{\epsilon\to 0}\langle k|\,T(E+i\epsilon)\,|k\rangle\,, \tag{2.2}$$

where E is, in general, independent of k, and

$$T(z) = V + VG^0(z)T(z) \tag{2.3a}$$

$$= V + VG(z)V \tag{2.3b}$$

is the T operator. In Eq. (2.3a) $G^0(z) = (z - H^0)^{-1}$ is the unperturbed Green's operator and $G(z)$ is the full Green's operator $(z-H)^{-1}$, where $H = H_0 + V$, V being the scattering potential. Additionally, $H^0|k\rangle = k^2/2|k\rangle$, $|k\rangle$ being the unperturbed scattering state. The analytic structure of the off-shell T-matrix element $T_k(z)$ as a function of the complex energy z for fixed k is determined by the analytic properties of $G(z)$ and schematically indicated in Fig. 1 for the e^+-H problem. We note in passing that the analytic properties of the amplitude $f(k=\sqrt{2E})$ can be considerably more complicated.[19] Schlessinger and Schwartz[8] noted that $T_k(E)$ (E real) could be easily computed for $E<\tilde{E}$, $\tilde{E}$ being the lowest bound state of H, using the Kohn principle which is, in this case, equivalent to

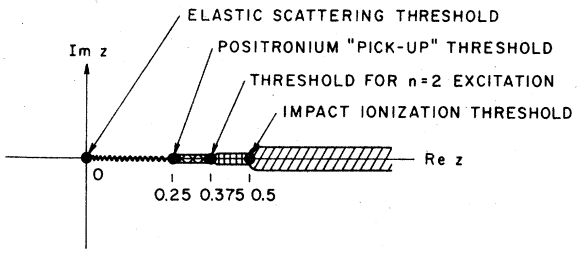

FIG. 1. Cut structure for the off-shell T-matrix for the case of e^+–H scattering. The analytic structure of this off-shell amplitude is determined by that of the resolvent $\langle(z-H)^{-1}\rangle$, which, in this case, has only cuts as there are no bound states of the composite three-body system. Thresholds (branch points) are at the ground and excited states of the possible bound two-particle subsystems (e^--H$^+$) and (e^+-e^-). For convenience we have chosen the zero of energy to correspond to the ground state of the H atom with a zero kinetic energy positron. An unusual feature of the e^+-H (1s) system is that the lowest inelastic threshold corresponds to the rearrangement (pick-up) $e^+ + \mathrm{H}\,(1s) \to \mathrm{H}^+ + \mathrm{P}\,(1s)$, where P (1s) is the ground state of positronium.

writing

$$\overline{T}(E) = V + V[1/(E-\overline{H})]V\,, \tag{2.4}$$

where $\overline{H}$ is a matrix representation of H in a finite subset of a complex discrete set of L^2 basis functions. Equation (2.4) may be rewritten as a matrix spectral resolution

$$\overline{T}(z) = V + \sum \frac{V|\tilde{\chi}_1\rangle\langle\tilde{\chi}_1|V}{z-\tilde{E}} \tag{2.5}$$

in terms of the matrix eigenvalue $\tilde{E}_1$ and $|\tilde{\chi}_1\rangle$:

$$\overline{H}\,|\tilde{\chi}_1\rangle = \tilde{E}_1\,|\tilde{\chi}_1\rangle i = 1, \cdots, N\,, \tag{2.6}$$

N being the dimensionality of the matrix representation. The representation of Eq. (2.5) is clearly not valid at scattering energies, as matrix elements of $V(E-\overline{H})^{-1}V$ are real even where H has a continuous spectrum—that is, the discretized Green's function $(E-\overline{H})^{-1}$ does not have the cuts of $(E-H)^{-1}$ itself. However, Schlessinger and Schwartz[8] were able to take values of $\langle k|\,T(E)\,|k\rangle$ from the negative real energy axis and to analytically continue them to the positive axis in the appropriate $E+i\epsilon$ limit via a simple square root uniformization and numerical rational fraction analytic continuation. McDonald and Nuttall[20] and Doolen *et al.*,[10] again using a version of the Kohn principle, in effect noted that a possibly better procedure would be to calculate

$$\overline{T}(z) = V + V[1/(z-\overline{H})]V \tag{2.7}$$

at complex energies close to desired scattering energy, but far enough from the real axis to avoid the spurious poles of $(z-\overline{H})^{-1}$. They thus computed an "extrapolated" T-matrix element as

$$\langle k|\,T(E+i\epsilon)\,|k\rangle \cong \lim_{q\to 0}{}' \langle k|\,\overline{T}\,[z=\tfrac{1}{2}(k+iq)^2]\,|k\rangle\,, \tag{2.8}$$

where lim′ implies that only values of q large enough to avoid spurious behavior of $\overline{T}(z)$ are included as input to the numerical limiting procedure. Typical extrapolation input data for the e^+-H case are shown in Fig. 2 of Ref. 10, where it is clear that the method is subject to computational noise, due to the convenient, but unfortunately approximate L^2 discretization of H. The power of the Schlessinger-Nuttall idea lies in the fact that, for multiparticle problems, amplitudes (presumably both elastic and inelastic) may be calculated above the breakup threshold, without detailed specification of channels and their corresponding boundary conditions, at least as long as one stays away from thresholds. Schlessinger was unable to calculate amplitudes above the breakup threshold for e^--H scattering because of numerical instabilities in the rational fraction

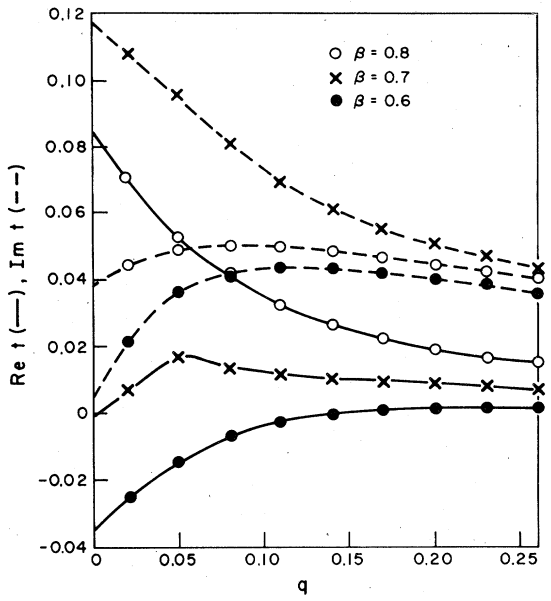

FIG. 2. Extrapolated T-matrix results for e^+-H$(1s)$ f-wave scattering for $k=1.4$ a.u. The f-wave amplitude is quite small when compared to the extrapolation error in both Ret and Imt. The moment method was also relatively poorly behaved for this partial wave; however, as shown in Table III, sensible results may be obtained.

continuation although these may have been avoided by the use of more sophisticated uniformization techniques.[21] Doolen *et al.*[10] have successfully applied the extrapolation techniques to compute the s-wave elastic amplitude for e^+-H scattering below and above the impact-ionization (breakup) thresholds. However, to obtain total and differential e^+-H cross sections one needs a large number of partial waves, and, as the numerical values of real and imaginary higher partial-wave amplitudes become quite small, the errors introduced by the extrapolation rapidly become larger than the amplitudes themselves. This is illustrated in Fig. 2 reproduced from Ref. 3, where an attempt was made to calculate the elastic e^+-H f-wave amplitude by T-matrix extrapolation.

III. MOMENT T-MATRIX METHOD

In this section we introduce moment techniques which allow direct calculation of the discontinuity of the off shell $(z \neq k^2/2)$ T-matrix element, $T_k(z) = \langle k|T(z)|k\rangle$, across the cuts on the real axis (see Fig. 1). Knowledge of this discontinuity, which is proportional to $\mathrm{Im}T_k(E+i\epsilon)$ allows construction of $\mathrm{Re}T_k(E+i\epsilon)$ via a dispersion (Hilbert transform) relationship between the real and imaginary parts of $T_k(E+i\epsilon)$. Direct construction of the discontinuity avoids the continuation and extrapolation procedures of Sec. II, and appears to be numerically more stable. It suffers from the same disadvantage as the off-shell methods of Sec. II in that the calculation of $\mathrm{Im}T_k(E+i\epsilon)$ and subsequent calculation of $\mathrm{Re}T_k(E+i\epsilon)$ must be begun anew for each value of k.

A. Calculation of Im $T_k(E+i\epsilon)$

Writing of the spectral resolution of the multichannel Green's function $(z-H)^{-1}$ in the condensed form

$$\frac{1}{z-H} = \int_0^\infty \frac{|\chi(E)\rangle\langle\chi(E)|}{z-E}dE \equiv \sum_\alpha \int_{E_\alpha^{\text{thresh}}}^\infty \frac{|\chi_\alpha(E)\rangle\langle\chi_\alpha(E)|}{z-E_\alpha}dE \tag{3.1}$$

where α denotes a channel, we have

$$T_k(z) = \langle k|V|k\rangle = \int_0^\infty \frac{\langle k|V|\chi(E')\rangle\langle\chi(E')|V|k\rangle}{z-E'}dE' \tag{3.2}$$

which may be rewritten in terms of the positive real density

$$\rho_k(E) \equiv |\langle k|V|\chi(E)\rangle|^2 \tag{3.3}$$

as

$$T_k(z) = \langle k|V|k\rangle = \int_0^\infty \frac{\rho_k(E')dE'}{z-E'} \tag{3.4}$$

or, in the $E+i\epsilon$ limit

$$T_k(E+i\epsilon) = \langle k|V|k\rangle + P\int_0^\infty \frac{\rho_k(E')dE'}{E-E'} - i\pi\rho_k(E). \tag{3.5}$$

Thus $\mathrm{Im}T_k(E+i\epsilon) = -\pi\rho_k(E)$, as the partial-wave Born term $\langle k|V|k\rangle$ is real. The discontinuity $T_k(E+i\epsilon) - T_k(E-i\epsilon)$ is thus $-2i\pi\rho_k(E)$, and knowledge of the discontinuity [i.e., $\rho_k(E)$] as a function of E (for fixed k) allows construction of $\mathrm{Re}T_k(E+i\epsilon)$ as

$$\mathrm{Re}T_k(E+i\epsilon) = \langle k|V|k\rangle + P\int_0^\infty \frac{\rho_k(E')dE'}{E-E'}. \tag{3.6}$$

Comparison of an approximate $\overline{T}_k(z) \equiv \langle k|\overline{T}(z)|k\rangle$ [see Eq. (2.5)] with $T_k(z)$ of Eq. (3.4) gives

$$\int_0^\infty \frac{\rho_k(E)dE}{z-E} \approx \sum_i \frac{\tilde{\rho}_k(\tilde{E}_i)}{z-\tilde{E}_i}, \tag{3.7}$$

where

$$\tilde{\rho}_k(\tilde{E}_i) \equiv |\langle k|V|\tilde{\chi}_i\rangle|^2, \tag{3.8}$$

illustrating the fact that we can interpret

$$\langle k|V[1/(z-\overline{H})]V|k\rangle \tag{3.9}$$

as a quadrature approximation[22] to

$$\langle k|\, V[1/(z-H)]\, V\,|k\rangle \tag{3.10}$$

itself, with weight ω_i and abscissas $\tilde{E}_i$, in the sense that we interpret

$$\int \frac{\rho_k(E)dE}{z-E} \approx \sum_i \frac{\omega_i\, \rho(\tilde{E}_i)}{z-\tilde{E}_i} = \sum_i \frac{\tilde{\rho}(\tilde{E}_i)}{z-\tilde{E}_i} \tag{3.11}$$

and thus

$$\rho(\tilde{E}_i) = \tilde{\rho}(\tilde{E}_i)/\omega_i\,. \tag{3.12}$$

Equation (3.12) implies that if we know the quadrature weight ω_i, associated with the particular discretization used to convert H to $\bar{H}$, we can compute $\rho(\tilde{E}_i)$ at the points $\tilde{E}_i$ (which usually cover enough of the real axis to make interpolation possible) and thus the discontinuity of $T_k(z)$ across the real axis. However, for an arbitrary basis the ω_i are not know *a priori*. However, the fact that a quadrature is implicit in the discretization allows extraction of *moments* of the positive definite distribution $\rho_k(E)$:

$$\sigma_n \equiv \int E^{-n}\rho_k(E)\,dE \cong \sum_i \omega_i \tilde{E}_i^{-n}\rho_k(\tilde{E}_i) = \sum_i \tilde{E}_i^{-n}\tilde{\rho}_k(\tilde{E}_i) \tag{3.13}$$

allowing computation of approximate moments from the $\tilde{\rho}_k(\tilde{E}_i)$, which are known. In an actual calculation a finite number of these moments will converge (usually the lower-order ones first) as a function of the basis set, and represent a smoothing of the discretized distribution $\tilde{\rho}_k(\tilde{E}_i)$ $i=1,\ldots,N$. This may seem like meager progress but, as seen in Secs. III B and III C, sensible approximations to $\rho_k(E)$ [and thus $\mathrm{Im}\,T_k(E+i\epsilon)$] can be systematically extracted from these converged moments.

B. Stieltjes extraction of Im T_k $(E+i\epsilon)$

The approximate moments

$$\tilde{\sigma}_n(k) = \sum_i \tilde{E}_i^{-n}\tilde{\rho}_k(\tilde{E}_i) \tag{3.14}$$

calculated from the discretized distribution $\tilde{\rho}_k(\tilde{E}_i)$ may be inverted by the Stieltjes imaging procedure developed by Langhoff and co-workers.[14] The converged moments $\tilde{\sigma}_n(k)(n=1,\cdots,M, M\ll N)$ approximate the moments

$$\sigma_n = \int_0^\infty E^{-n}\rho_k(E)\,dE \tag{3.15}$$

of a positive definite distribution $\rho_k(E)$. Using standard Gaussian quadrature ideas we see that the moments yield quadrature points (ϵ_n^ρ) weights (ω_n^ρ) $(n=1,\cdots,M/2)$ for Gaussian integration over $\rho_k(\epsilon)$ as a weight function

$$\int_0^\infty \rho_k(E) f(E)\,dE \cong \sum_{n=1}^{M/2} \omega_n^\rho f(\epsilon_n^\rho)\,, \tag{3.16}$$

where the integration is exact if $f(E)$ is a polynomial (in E^{-1}) of order $M+1$. In particular, we have the exact result

$$\int_0^\infty \rho_k(E)\,dE = \sum_n \omega_n^\rho\,, \tag{3.17}$$

suggesting that

$$\rho_k^{\mathrm{cumul}}(\epsilon) \equiv \int_0^\epsilon \rho_k(E)\,dE = \sum_{n=1}^{n^*} \omega_n^\rho\,, \tag{3.18}$$

where n^* is chosen such that $\epsilon_{n^*}^\rho \leq \epsilon \leq \epsilon_{n^*+1}^\rho$. This provides a histogram representation of the cumulative weight function $\rho^{\mathrm{cumul}}(\epsilon)$, which may be interpolated to give $\rho_k^{\mathrm{cumul}}(\epsilon)$ as a smooth function of ϵ, $\rho_k(E)$ itself being obtained as

$$\rho_k(E) = \frac{d}{d\epsilon}\rho_k^{\mathrm{cumul}}(\epsilon)\Big|_{\epsilon=E}\,. \tag{3.19}$$

This has proved to be a highly successful inversion procedure in numerous applications.[14]

One might ask why the moment extraction step is necessary, as one might feel that

$$\rho_k^{\mathrm{cumul}}(\epsilon) \cong \sum_{i=1}^{i^*} \tilde{\rho}_k(\tilde{E}_i)\,, \tag{3.20}$$

where i^* is chosen such that $\epsilon_{i^*} \leq \epsilon < \epsilon_{i^*+1}$ would give a suitable approximation to $\rho_k^{\mathrm{cumul}}(\epsilon)$. The difficulty is that the distribution $\tilde{\rho}_k(\tilde{E}_i)$ resulting from an arbitrary discretization is not smooth enough to allow the unambiguous interpolation of ρ_k^{cumul} which is needed to perform the differentiation needed to construct $\rho_k(E)$, via Eq. (3.19). Taking a small $(M\ll N)$ number of moments smooths the primitive distribution $\tilde{\rho}_k(\tilde{E}_i)$ to allow extraction of an approximation to $\rho_k(E)$. In the e^+-H problem the above Stieltjes approximation was not always reliable, as $\rho_k^{\mathrm{cumul}}(\epsilon)$ varied by several orders of magnitude over a very small range of energies (often *in between* two of the $\tilde{E}_n$), making interpolation of the histogram approximation ambiguous, and suggesting that an alternative extraction procedure was needed.

C. Derivative rule extraction of Im T_k $(E+i\epsilon)$

An alternative technique[16,17] for extraction of an approximation to $\rho_k(E)$ from the approximate moments σ_n $(n=1,\ldots,M, M\ll N)$ utilizes the fact that if ϵ_n^ρ and ω_n^ρ are, respectively, the Gauss quadrature abscissas and weights for integration with weight function ρ, smooth interpolation of the ϵ_n^ρ as a function of n, gives (see Appendix A)

$$\omega_n^{eq} \equiv \frac{d}{d\xi}\epsilon_\xi^\rho\Big|_{\xi=n} = \frac{\omega_n^\rho}{\rho(\epsilon_n^\rho)}, \tag{3.21}$$

defining the "equivalent quadrature" weight ω_n^{eq}, which is the quadrature weight divided by the weight function. Thus an approximation to $\rho_k(\epsilon)$ at energy ϵ_n^ρ is given by

$$\rho_k(\epsilon_n^\rho) = \omega_n^\rho \Big/ \frac{d}{d\xi}\epsilon_\xi^\rho\Big|_{\xi=n} = \frac{\omega_n^\rho}{\omega_n^{eq}} \tag{3.22}$$

as the ω_n^ρ as well as the ϵ_n^ρ are directly determined from the moments. Extraction of $\rho_k(\epsilon_n^\rho)$ via this method requires, as does the Stieltjes imaging process, a numerical interpolation followed by a numerical differentiation. If the ϵ_n^ρ are regularly spaced, and if the ω_n^ρ are not too rapidly varying, both methods give comparable results. However, if, as is the case for e^+-H scattering, the ω_n^ρ are very strong functions of n, while the ϵ_n^ρ are relatively smooth functions of n, the derivative technique offers a reasonable approximation scheme, whereas the Stieltjes method fails totally.

D. Construction of Re T_k $(E+i\epsilon)$

$\mathrm{Re}T_k(E+i\epsilon)$ is constructed via a quadrature approximation to the dispersion representation of Eq. (3.6),

$$\begin{aligned}\mathrm{Re}T_k(E+i\epsilon) &= \langle k|V|k\rangle \\ &\quad + P\int_0^\infty \frac{\langle k|V|\chi(E')\rangle\langle\chi(E')|V|k\rangle}{E-E'}\,dE' \\ &= \langle k|V|k\rangle + P\int_0^\infty \frac{\rho_k(E')\,dE'}{E-E'}.\end{aligned} \tag{3.23}$$

The positive density $\rho_k(E)$ is available from the Stieltjes and/or derivative rule at the points ϵ_n^ρ, and is numerically interpolated as a function of E. The principal valued integral is then carried out at energy E by adding and subtracting $\rho_k(E)$ in the integrand (dispersion correction[23]):

$$\begin{aligned}\mathrm{Re}T_k(E+i\epsilon) &= \langle k|V|k\rangle + \int_0^\infty \frac{[\rho_k(E')-\rho_k(E)]}{E-E'}\,dE' \\ &\quad + \rho_k(E)P\int_0^\infty \frac{dE'}{E-E'}.\end{aligned} \tag{3.24}$$

As the first integral in Eq. (3.24) is no longer singular at $E=E'$ [provided that $\rho_k(\epsilon)$ satisfies an appropriate Lipshiftz condition[23]] we can perform a numerical quadrature. It is particularly convenient to use the quadrature weight and abscissas determined from the moments of $\rho_k(E)$ itself, namely, the $(\omega_n^\rho, \epsilon_n^\rho)$, and the equivalent quadrature weights ω_n^{eq}, as determined in Sec. III C. Thus

$$\begin{aligned}\mathrm{Re}T_k(E+i\epsilon) &\cong \langle k|V|k\rangle + \sum_{n=1}^{M}\frac{\omega_n^\rho}{E-\epsilon_n^\rho} \\ &\quad + \rho_k(E)P\int_0^\infty \frac{dE'}{E-E'} - \sum_{n=1}^{}\frac{\omega_i^{eq}}{E-\epsilon_n^\rho}.\end{aligned} \tag{3.25}$$

In Eq. (3.25) the integral $P\int_0^\infty dE'\,(E-E')^{-1}$ diverges, unless a high energy cutoff is imposed. However, the quadrature itself imposes such a cutoff which we denote as E^{max}. E^{max} may be determined by enforcing the condition

$$\int_0^{E_{max}} \frac{dE'}{E+E'} = \sum_{n=1}^{M}\frac{\omega_n^\rho}{E+\epsilon_n^\rho}. \tag{3.26}$$

This choice of E^{max} gave excellent results when applied to model problems[3] and, as will be seen in the following section excellent agreement with previous e^+-H amplitudes, in the cases where comparison is possible. The final working approximation for $\mathrm{Re}T_k(E+i\epsilon)$ is thus

$$\begin{aligned}\mathrm{Re}T_k(E+i\epsilon) &= \langle k|V|k\rangle + \sum_{n=1}^{M}\frac{\omega_n^\rho}{E-\epsilon_n^\rho} \\ &\quad + \rho_k(E)P\int_0^{E_{max}} \frac{dE'}{E-E'} - \sum_{n=1}^{M}\frac{\omega_n^{eq}}{E-\epsilon_n^\rho}\end{aligned} \tag{3.27}$$

with E^{max} determined from Eq. (3.26). As we are working with an off-shell amplitude Eq. (3.27) only approximates $\mathrm{Re}T_k(E+i\epsilon)$ for[18] $E=\frac{1}{2}k^2$ implying that the determination of moments and subsequent extraction of $\{\omega_n, \epsilon_n^\rho\}$ and ω_n^{eq} must be entirely redone as a function of k. This is a disappointingly tedious procedure, but apparently a necessity, as totally off-shell methods, such as the Fredholm method,[9] which attempt to calculate the amplitudes at all energies from a single major step, failed when applied to the e^+-H problem.[3] We do note, however, that the construction of the eigenvectors $|\tilde{\chi}_i(\tilde{E}_i)\rangle$ need only be performed once for each choice of basis, as the diagonalization of $\bar{H}$ is independent of k.

IV. CALCULATIONAL METHODS

In Sec. IV A (and Appendix B) we briefly review calculational matrix elements of H, and determination of the eigenvalues and eigenvectors. Section IV B contains an outline of the moment and interpolatory methods used to extract $\mathrm{Im}T_k(E+i\epsilon)$, followed by two examples in Sec. IV C.

A. Matrix elements and matrix manipulations

The two-particle fixed nucleus Hamiltonian

$$H = -\frac{\nabla_1^2}{2} - \frac{\nabla_2^2}{2} - \frac{1}{r_{12}} - \frac{1}{r_1} + \frac{1}{r_2}, \tag{4.1}$$

where $1 = e^-$, $2 = e^+$, and $r_{12} = |\vec{r}_1 - \vec{r}_2|$, was discretized in the nonorthogonal Hylleraas basis[24]

$$\Phi_i(\vec{r}_1, \vec{r}_2) = r_1^{n_1^i} r_2^{n_2^i} r_{12}^{n_{12}^i} \exp(-\alpha r_1 - \beta r_2)\, Y_{l_1 l_2 L}(\Omega_1, \Omega_2), \tag{4.2}$$

where for states of parity $(-1)^L$, $l_1 + l_2 = L$.[25] Calculation of $\langle \phi_i | H | \phi_j \rangle$ and $\langle \phi_i | \phi_j \rangle$ proceed as in Ref. 24, resulting in a secular problem of the form $(\bar{H} - S\tilde{E}_i)\tilde{\chi}_i(\tilde{E}_i) = 0$ for each choice of nonlinear parameters α, β and for each total angular momentum L. In order to build up the static exchange cut in $(z - H)^{-1}$ α was fixed at its hydrogenic value ($\alpha = 1$) and a large number of functions of the type $n_1 = 0$, $n_{12} = 0$, and $n_2 = 0 \to N$ were included for values of N ranging up to 13 and 14.[26] Polarization and correlation were then included by systematic inclusion of larger values of n_1 and n_{12}. Calculations were carried out over a range of basis set sizes and values of β to check convergence. Due to the large number of functions containing high powers of $r_2^{n_2}$ serious numerical problems arose in solution of the secular problem. The Givens[27] technique proved unstable, and the QZ algorithm[28] for solution of the generalized eigenproblem $AX = \lambda Bx$ was finally chosen as a compromise between speed, storage, and accuracy.

Construction of the matrix elements

$$\langle k | V | k \rangle \equiv \langle j_l(kr_2)\phi_{1s}(r_1) | + 1/r_2 - 1/r_{12} | \times j_l(kr_2)\phi_{1s}(r_1) \rangle \tag{4.3}$$

and

$$\langle k | V | \phi \rangle \equiv \langle j_l(kr_2)\phi_{1s}(r_1) | + 1/r_2 - 1/r_{12} \times \phi_i(\vec{r}_1, \vec{r}_2) \rangle, \tag{4.4}$$

$\phi_{1s}(r_1)$ being the hydrogenic ground-state wave

TABLE I. The matrix eigenvalues E_i and the $\tilde{\rho}_k(\tilde{E}_i)$ for s-wave scattering at $k = 1.1$ a.u. A 105-term Hylleraas basis with $\alpha = 1.0$, $\beta = 0.8$ was used to discretize H. Energy is in rydbergs.

i	$\tilde{E}_i$	$\tilde{\rho}_k(\tilde{E}_i)$	i	$\tilde{E}_i$	$\tilde{\rho}_k(\tilde{E}_i)$	i	$\tilde{E}_i$	$\tilde{\rho}_k(\tilde{E}_i)$
1	0.017637	2.888 936(−04)	36	2.583 566	1.074 242(−02)	71	6.516 462	6.438 273(−03)
2	0.079 157	9.657 560(−04)	37	2.603 927	1.805 086(−04)	72	6.634 387	5.438 393(−02)
3	0.206 514	2.292 725(−03)	38	2.752 572	1.293 384(−05)	73	7.027669	1.356 834(−04)
4	0.448 177	4.346 923(−03)	39	2.798 047	2.064 499(−02)	74	7.122306	6.944 094(−05)
5	0.577 953	1.186 408(−04)	40	2.861386	4.767 174(−03)	75	7.278 887	7.223 282(−02)
6	0.827 163	3.143 996(−04)	41	2.910 715	1.537 421(−02)	76	7.575 754	6.302 850(−02)
7	0.866 161	2.494 854(−06)	42	3.072 036	7.221 960(−03)	77	7.652638	1.575 537(−01)
8	0.901803	1.845 345(−04)	43	3.139464	1.798 908(−02)	78	8.093373	2.833 812(−02)
9	0.921259	9.024 511(−03)	44	3.221670	4.980 644(−02)	79	8.368 530	1.632 732(−05)
10	1.039175	4.359469(−04)	45	3.323630	6.221 150(−02)	80	8.593 575	1.172 897(−01)
11	1.085255	1.356 574(−03)	46	3.341645	1.242 994(−02)	81	8.798668	1.233 493(−03)
12	1.150 753	1.148 011(−06)	47	3.405344	3.437 028(−03)	82	9.522294	1.462 771(−03)
13	1.225179	6.957470(−05)	48	3.557 933	9.070 760(−03)	83	9.904670	3.318 883(−05)
14	1.287269	1.099 137(−04)	49	3.628 728	5.156 720(−02)	84	10.152635	1.888 226(−04)
15	1.364 500	3.153 834(−04)	50	3.690 376	1.563 880(−02)	85	10.922446	4.469 131(−05)
16	1.385889	2.711 576(−05)	51	3.780694	3.099 930(−02)	86	11.060 756	1.491 890(−05)
17	1.504 550	1.220 458(−04)	52	3.874 548	5.514 746(−03)	87	11.976 649	8.112 760(−03)
18	1.544673	1.220 440(−04)	53	3.970 333	7.214 416(−03)	88	12.347 758	3.827 408(−03)
19	1.561 114	1.042 694(−08)	54	4.137 761	4.385 912(−03)	89	13.360 139	2.041 041(−04)
20	1.595 976	6.357 828(−04)	55	4.261560	6.134 475(−03)	90	14.177 703	1.654 196(−02)
21	1.631269	2.700 966(−05)	56	4.331396	1.931 241(−04)	91	14.964 962	6.746 771(−03)
22	1.714 108	4.193637(−04)	57	4.496 710	7.700 816(−04)	92	15.115440	1.385 386(−04)
23	1.811686	1.464 138(−03)	58	4.634 734	1.345 384(−03)	93	15.501294	9.219 767(−06)
24	1.885 752	3.559485(−04)	59	4.773 744	1.529 399(−02)	94	16.872495	2.484 770(−02)
25	1.939691	2.220 712(−03)	60	4.976 983	2.010 815(−05)	95	17.100 950	8.952668(−04)
26	1.986 838	1.637 859(−02)	61	5.015437	1.912408(−05)	96	19.201838	8.278 173(−05)
27	2.011373	1.056 815(−02)	62	5.156 052	8.075 326(−03)	97	19.630 367	1.079 817(−03)
28	2.039 163	2.679 216(−03)	63	5.297 794	1.728 911(−02)	98	19.823 224	1.097 637(−01)
29	2.168 267	4.278 626(−03)	64	5.567 123	6.601 771(−03)	99	21.098 758	6.061 541(−02)
30	2.218 557	1.015699(−03)	65	5.685498	2.801 195(−03)	100	21.945 342	3.306 382(−02)
31	2.275 752	7.532 180(−04)	66	5.838 943	1.186 487(−02)	101	24.743 037	1.919841(−01)
32	2.322621	4.270 564(−03)	67	5.992 070	6.371418(−03)	102	25.273 525	5.635870(−02)
33	2.396 869	6.703 789(−03)	68	6.115 129	2.569 081(−02)	103	25.951 542	6.825 042(−05)
34	2.441 982	8.182 292(−04)	69	6.234478	4.984 251(−02)	104	31.031432	1.068 242(−01)
35	2.533 051	2.882 810(−05)	70	6.274 614	7.601 954(−02)	105	37.861 714	3.043 076(−01)

TABLE II. Quadrature abscissas (ϵ_i^ρ), weights (ω_i^ρ), and equivalent quadrature weights ω_i^{eq} obtained from 16 moments of the raw distribution of $\tilde{E}_i$ and $\tilde{\rho}_k(\tilde{E}_i)$ shown in Table I for two different values of the mapping parameter $S2$ [see text]. The weights and abscissas are now smoothly varying functions of i allowing extraction of $\rho(E)$ via the derivative rule [Eq. (3.22)].

i	ϵ_i^ρ	ω_i^I	$\omega_i^{eq} = \frac{\omega_i^\rho}{\rho(E_i)}$
		$S2 = 0.8$	
1	0.0277	5.2648(−04)	4.7185(−02)
2	0.1318	1.8525(−03)	1.6788(−01)
3	0.3529	4.2239(−03)	2.9485(−01)
4	0.8483	1.1617(−02)	8.2245(−01)
5	2.1891	1.0279(−01)	1.6681
6	3.8884	4.2076(−01)	2.1381
7	8.3155	6.9347(−01)	8.6686
8	29.8703	8.2342(−01)	4.1725(+01)
		$S2 = 0.5$	
1	0.0186	3.1080(−04)	3.0721(−02)
2	0.0849	1.0695(−03)	1.0620(−01)
3	0.2270	2.6631(−03)	1.9321(−01)
4	0.5304	6.0449(−03)	4.4579(−01)
5	1.2486	2.2155(−02)	1.1257
6	3.0593	3.5163(−01)	2.4792
7	7.1377	7.8938(−01)	7.7583
8	28.4302	8.8541(−01)	4.3487(+01)

function, which are needed in construction of approximations to $T_k(z)$, is outlined in Appendix B.

B. Moment-extraction techniques

Finding a reliable technique for extracting scattering information from the moments $\tilde{\sigma}_n$ of the raw distribution $\tilde{\rho}_k(\tilde{E}_i)$ proved to be difficult. The energy interval $(0, \infty)$ was mapped onto $(-1, +1)$ via the transformation $x = (E - S2)/(E + S2)$, where $S2$ is a variable in the interval $(0, \infty)$. Changing $S2$ weights differing parts of the interval, rather than the low-energy region sampled most strongly by the raw inverse power moments $\tilde{\sigma}_n$. The moment problem was solved in x space (as a function of $S2$) via the generalized technique of Sack and Donovan,[29] and the resulting x-space quadrature points and weight mapped back to the interval $(0, \infty)$ to yield the ϵ_n^ρ and ω_n^ρ. Changing $S2$ gives different sets of ϵ_i^ρ and ω_n^ρ which yielded different approximations to $\mathrm{Im}T_k(E + i\epsilon)$ at the different energies ϵ_i^ρ. Variation of $S2$ thus allows $\mathrm{Im}T_k(E + i\epsilon)$ to be obtained at a large number of energies ϵ_n^ρ, from a calculation in a single basis. The ϵ_i^ρ from a single value of $S2$ turned out to range over energies from 0.1 to 3 Ry (except for the s-wave case where the

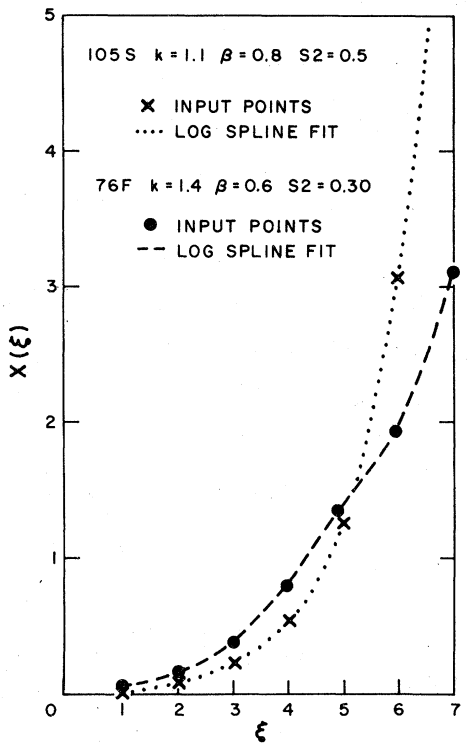

FIG. 3. Interpolation of the quadrature abscissas (obtained from the moment analysis) which are needed to compute the equivalent quadrature weights ω_n^{eq}. The dotted line shows an interpolation for the s-wave amplitude, resulting in the values of Imt shown in Fig. 4. In this case the interpolation is satisfactory. The dashed line shows a similar interpolation of f-wave quadrature abscissas: points as $\xi = 2$, 3, 4, 5 do not interpolate "smoothly" (i. e., there seems to be inflection points in the interpolated curve) leading to the scatter in Imt shown in Fig. 5.

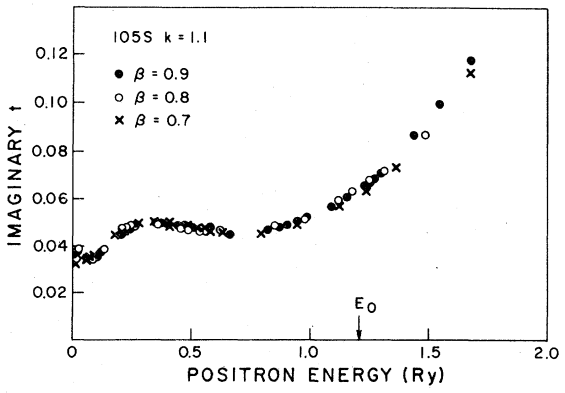

FIG. 4. Im$t_k(E + i\epsilon)$ for a range of E for three different values of the nonlinear parameter β for a value of $k = 1.1$ a.u. Results for many different mappings (values of $S2$) are shown. Im $t_k(E + i\epsilon)$ is reasonably well converged.

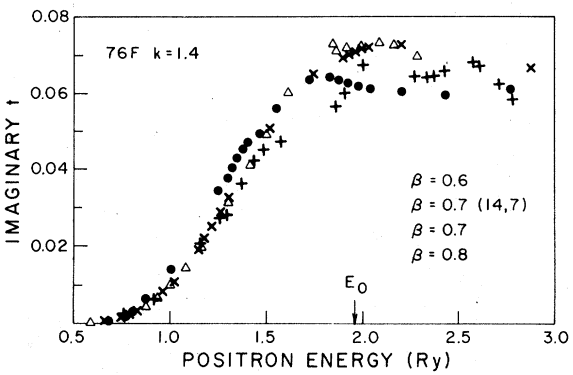

FIG. 5. $\mathrm{Im}\, t_k(E+i\epsilon)$ as a function of E for several values of the nonlinear parameter β, for $k=1.4$ (a.u.). This was a worst case in terms of convergence with respect to basis size β and mapping parameter $S2$, and indicates that $\mathrm{Im}\, t_k[E_0+i\epsilon=(k^2/2)+i\epsilon]$ is probably only determined to about 15%–20%. See Table III for a numerical summary of calculation of the f-wave cross section.

highest ϵ_i^o were about 8 and 30 Ry), the necessary interpolation to obtain the derivative equivalent weights ω_i^{eq} [Eq. (3.21)] was unstable because of this large range of magnitudes, thus interpolation was performed via spline interpolation of the $\ln(\epsilon_i^o)$, the smooth functions $i=1,\ldots,M$.

C. Examples

To give a feeling for the quality of data obtained from the moment T-matrix method, we give some illustrative results for a good case (s-wave scattering) and for a particularly bad case (f-wave scattering).

1. *s-wave amplitude*

Table I gives the raw $\tilde{E}_i$ and $\tilde{\rho}_k(\tilde{E}_i)$ obtained from a calculation involving 105 Hylleraas $L=0$ basis for $k=1.1$ a.u., $\alpha=1.0$, $\beta=0.8$. Inspection of the $\tilde{\rho}_k(\tilde{E}_i)$ shows a roughness which must be smoothed to obtain sensible approximation to $\rho_k(E)$ itself. The ϵ_i^o and ω_i^o obtained from the moment analysis are shown in Table II for $S2=0.5$ and $S2=0.8$, while the log spline interpolation used for the $S2=0.5$ data is shown in Fig. 3. This is a favorable case as the $\ln(\epsilon_i^o)$ plot is smooth and monotonic, allowing accurate interpolation. The family of curves obtained from various mappings ($S2$ values) and for different choices of nonlinear parameter β is shown in Fig. 4, where we focus attention on the value of $\mathrm{Im}t_k$ at $\frac{1}{2}k^2=E=0.605$ a.u. In this figure, and in what follows,

$$t_k(E+i\epsilon)\equiv -k[\langle k\,|\,V\,|\,k\rangle + \langle k\,|\,VG(E+i\epsilon)V\,|\,k\rangle\,]\,|_{E=k^2/2} \tag{4.5}$$

rather than $T_k(E+i\epsilon)$ is shown. This choice follows from the fact that $t_k=e^{i\delta}\sin\delta$, and thus is simply related to the phase shift δ. In this case, using the data from calculations with $\beta=0.7$, 0.8, and 0.9 and $S2$ ranging from 0.2 to 0.8, we conclude that $\mathrm{Im}t_k=0.065\pm0.003$ and $\mathrm{Re}t_k=-0.195\pm0.003$ for $k=1.1$. This fairly well converged result is at an energy above the breakup threshold, but is typical of the result obtained above and below the inelastic region in favorable cases.

2. *f-wave amplitude*

The corresponding interpolation and $\mathrm{Im}t_k(E+i\epsilon)$ obtained for f-wave scattering from a 76-term basis at $k=1.4$ (a worst case) are shown in Figs. 3 and 5, respectively. The interpolation is not smooth for this value of β, resulting in uncertainty in the derivative weights. This uncertainty manifests itself strongly in the results shown in Fig. 5 suggesting that $\mathrm{Im}t_k(E+i\epsilon)$ is only determined to above 10% at $E=\frac{1}{2}k^2=0.98$ a.u. However, even in this case things are not as bad as they seem. Typical extrapolation results are shown for com-

Table III. Examples of convergence of the moment T-matrix method and T-matrix extrapolation methods. The case at hand is a calculation of the f wave e^+-H(1s) elastic amplitude at a positron momentum $k=1.4$ (a.u.). This is a "worst case" for the moment method (see Figs. 3 and 5; results for $|t|^2$ are only good to ~15%. It is clear, however, that the extrapolation method has failed completely in this case (see Fig. 2).

	Moment method			Extrapolation method		
	Ret [a]	Imt	$\lvert t\rvert^2$	Ret	Imt	$\lvert t\rvert^2$
$\beta=0.8$	0.0241(7)	0.062(6)	0.0044	0.085(10)	0.040(10)	0.0088
$\beta=0.7$	0.0146(73)	0.071(73)	0.0052	0.000(10)	0.116(10)	0.0134
$\beta=0.6$	0.0027(10)	0.062(6)	0.0039	−0.032(10)	0.005(10)	0.00105

[a] The figures in parentheses indicates the estimated error in the last figure shown [e.g., 0.0146(73) ⇒ 0.0146 ± 0.0073]. The estimated errors in the moment method were calculated as the standard deviation of values obtained using at least five different mapping parameters. The estimates of the errors of the extrapolation results are visual, and were made from Fig. 2.

TABLE IV. s-wave e^+-H(1s) elastic phase shifts as a function of positron momentum k. Results of three separate moment T-matrix calculations (A,B,C) are compared with the variational results of Bhatia *et al.* (Ref. 4). Each of the T-matrix amplitudes is the average result of at least five mappings, with different $S2$: 16 moments were used.

k (a.u.)	A [a]	B [b]	C [c]	Bhatia
0.1	0.147	0.147	0.149	0.148
0.2	0.178	0.179	0.177	0.188
0.3	0.160	0.158	0.155	0.168
0.4	0.120	0.119	0.119	0.120
0.5	0.062	0.064	0.064	0.062
0.6	0.0015	0.003	0.003	0.004
0.7	−0.053	−0.051	−0.051	−0.051

[a] 105-term basis $\alpha = 1$, $\beta = 0.7$.
[b] 105-term basis $\alpha = 1$, $\beta = 0.8$.
[c] 105-term basis $\alpha = 1$, $\beta = 0.9$.

parison in Fig. 2, and the situation summarized in Table III. It is seen that the moment T-matrix method has given a moderately well-converged value of $|t_k|^2$ while the extrapolation methods have failed completely.

V. RESULTS

The motivation for development of the moment T-matrix method was to calculate amplitudes to the intermediate-energy region where a continuum of channels is open. However, to gain confidence in the reliability of the method we give results for low-energy scattering, where only the elastic channel is open. In this energy region we can compare with essentially exact variational results, and find that the method is easily reliable to about 5%, a more than acceptable error for extension past the breakup threshold. At the same time it is clear that the moment T-matrix method cannot compete with the high precision of the variational methods[4,7] in the case that only one channel is open.

Tables IV–VI give s-, p-, and d-wave phase shifts, in comparison with those obtained by variational techniques. The resulting partial wave cross sections, $\sigma_l = (4/k^2)(2l+1)|t_k^l|^2$, in units of πa_0^2, where t_k^l is the lth wave amplitude, are shown graphically in Figs. 6–8. It is clear that at relatively low energies ($k = 0.1, 0.2, 0.3$) the moment T-matrix method suffers in comparison with the variational work of Bhatia *et al.*[4] and Register and Poe.[7] This results from the fact that for all reasonable values of the mapping parameter $S2$, only one abscissa ϵ_i^ρ appears in the low-energy region ($k = 0.3$ is $E = 0.045$ a.u.) making interpolation treacherous. However, at somewhat higher k values the method is working well. Table VII displays f- and g-wave results. It is evident from the table that the adiabatic Dalgarno-Lynn[6] results are a moderately good representation at this point, and we have used the Dalgarno-Lynn phase shifts for $L = 5$ through 8 in construction of differential cross sections. Past $L = 8$ the Born[30] and Dalgarno-Lynn phase shifts are essentially identical, as is illustrated in Table VIII.

Converged differential cross sections

$$\frac{\partial\sigma}{\partial\Omega} = \frac{1}{k^2}\left|\sum_{l=0}^{\infty}(2l+1)t_k^l P_l(\cos\theta)\right|^2,$$

in units of a_0^2/sr, at $k = 0.4$ and 0.6 a.u., are shown in Figs. 9 and 10 followed by the total cross section as a function of energy in Fig. 11.

TABLE V. p-wave elastic e^+-H(1s) phase shift as computed by the moment T-matrix method (A, B, C) are compared with the extrapolated variational results of Armstead (Ref. 7) and Bhatia *et al.* (Ref. 4). Each of the T-matrix results employed 16 moments and is the average of at least five different mappings.

					Bhatia	
k (a.u.)	A [a]	B [b]	C [c]	Armstead	I [d]	II [e]
0.1	0.0073	0.0066	0.008	0.009	0.0076	0.0094
0.2	0.0321	0.033	0.032	0.032	0.0323	0.0338
0.3	0.064	0.063	0.065	0.065	0.0648	0.0665
0.4	0.098	0.095	0.097	0.102	0.0988	0.1016
0.5	0.130	0.128	0.128	0.132	0.1292	0.1309
0.6	0.155	0.160	0.154	0.156	0.153	0.1547
0.7	0.171	0.175	0.171	0.178	0.175	0.1799

[a] 87-term basis $\alpha = 1$, $\beta = 0.7$.
[b] 87-term basis $\alpha = 1$, $\beta = 0.8$.
[c] 87-term basis $\alpha = 1$, $\beta = 0.9$.
[d] 70-term basis.
[e] 168-term basis, extrapolated.

TABLE VI. d-wave elastic e^+-H phase shifts as calculated via the moment T-matrix method, as compared with the variational results of Register and Poe (RP) (Ref. 4) and the adiabatic Dalgarno-Lynn (DL) results (Ref. 6).

k (a.u.)	A [a]	B [b]	C [c]	RP	DL
0.1	0.00044	0.0003	0.0002	0.0013	0.0014
0.2	0.0050	0.0044	0.0037	0.0054	0.0056
0.3	0.0124	0.0124	0.0122	0.0125	0.0127
0.4	0.0235	0.0230	0.0226	0.0235	0.0225
0.5	0.0386	0.0396	0.0379	0.0389	0.0340
0.6	0.0587	0.0589	0.0588	0.0593	0.0462
0.7	0.0858	0.0854	0.0870	0.0863	0.0578

[a] 100-term basis, $\alpha = 1.0$, $\beta = 0.6$.
[b] 100-term basis, $\alpha = 1.0$, $\beta = 0.7$.
[c] 100-term basis, $\alpha = 1.0$, $\beta = 0.8$.

VI. SUMMARY

In the present paper we have developed a moment theory which allows direct construction of the total discontinuity of the off-shell T-matrix $T_k(z)$ across the real axis cuts. The method involves a projection of a Hilbert space discretization of the full resolvent, $(z-H)^{-1}$, onto the unperturbed scattering state $\Phi_{1s}(r_1)j_l(kr_2)$, and does not require detailed channel enumeration. The method was applied to e^+-H elastic scattering below the positronium pick-up threshold, 0.25-a.u. scattering energy, with good results producing s-, p-, d-, f-, and g-wave correlated phase shifts, and the resulting total and differential cross sections. The real power of the technique, however, lies in the ability to perform calculations at scattering energies *above* the impact ionization threshold. Results of such calculations are presented in the companion paper.[2]

ACKNOWLEDGMENTS

The support of this work by the NSF through Grant Nos. CHE77-16307 and PHY76-04761 and fellowship support to WPR from the J. S. Guggenheim Foundation, and the Council on Research and Creative Work of the University of Colorado, Boulder, are most gratefully acknowledged, as are most helpful conversations with P.W. Langhoff, T. Murtaugh, T. Rescigno, H.A. Yamani, E. J. Heller, and J. T. Broad. The authors are most grateful to P. G. Burke and A. J. Taylor from whose Hylleraas program our work grew.

APPENDIX A: DERIVATIVE RULE

Heller[16] suggested if $\{x_i\}$ and $\{\omega_i\}$ are a set of nth-order Gaussian quadrature weights and points for integration with respect to a weight function $\rho(x)$ [i.e., x_i are the zeros of the $(N+1)$st order polynomial orthogonal with respect to $\rho(x)$] then a "smooth" interpolation of the x_i to give $x(\xi)$, such that

$$x(\xi)\big|_{\xi=i} = x_i \tag{A1}$$

has the interesting and useful property that

$$\frac{d}{d\xi}x(\xi)\bigg|_{\xi=i} = \frac{\omega_i}{\rho(x_i)} \ , \tag{A2}$$

where ω_i is the quadrature weight, and $\rho(x_i)$ the

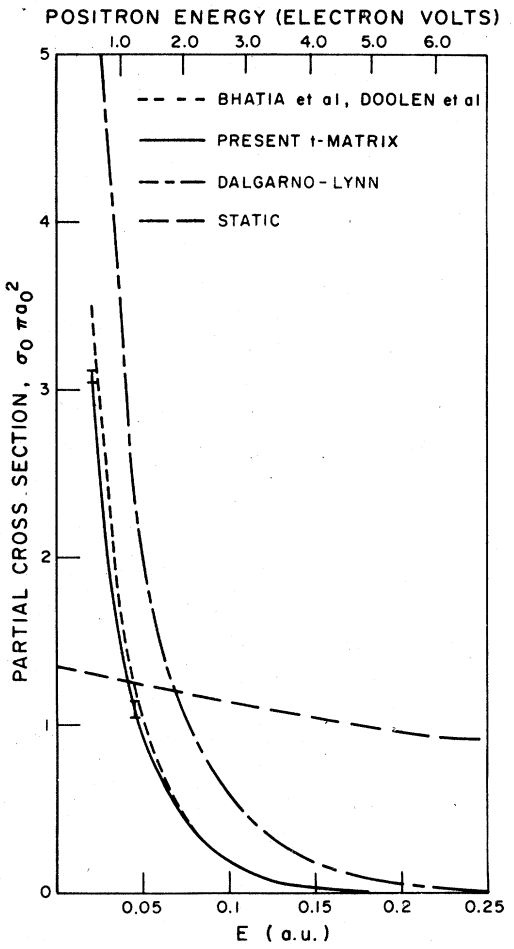

FIG. 6. s-wave partial elastic cross section for $e^+ + H(1s)$ at energies below the pick-up threshold at 0.25 (a.u.). Results are shown in the static and adiabatic (Dalgarno-Lynn) approximations, as well as those using fully correlated Hylleraas-type basis sets thus including polarization and correlation effects. The present moment T-matrix results are in excellent agreement with the previous correlated calculations of Bhatia *et al.* and Doolen *et al.* except at very low energies, where, as discussed in the text, the moment method suffers from the problem that the necessary interpolations become ill defined.

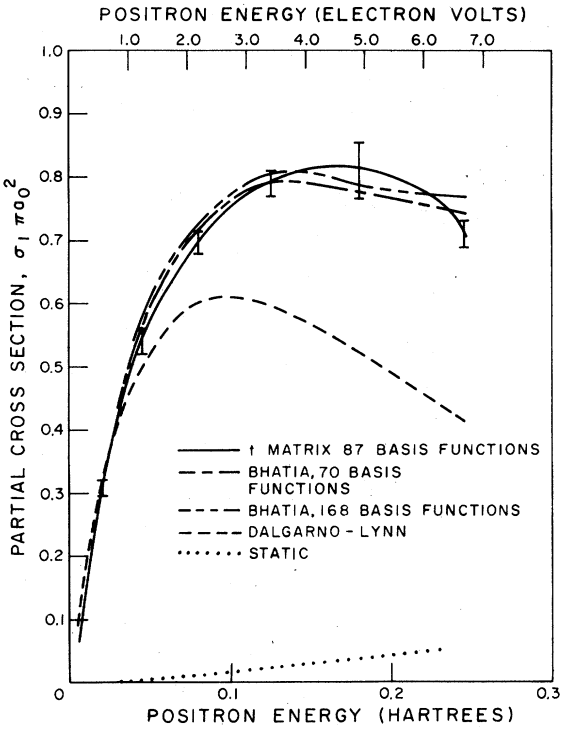

FIG. 7. p-wave partial e^+-H(1s) cross section below the pick-up threshold. The error bars indicate estimated error based on taking the standard deviation of results obtained from a large number of mappings. The moment T-matrix results compare well with the variational calculations of Bhatia.

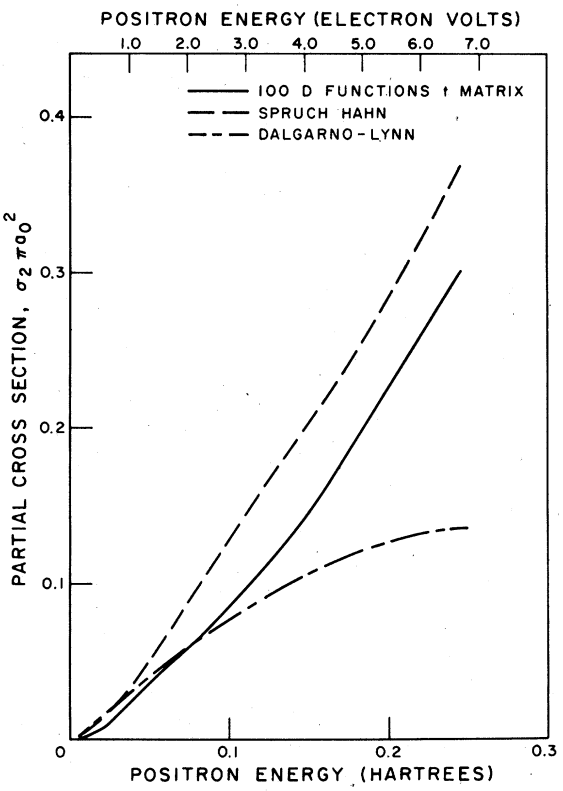

FIG. 8. d-wave partial elastic cross section for e^+-H(1s) scattering below the pick-up threshold. The results are compared with the adiabatic Dalgarno-Lynn results, and the partially correlated results of Sprach and Hahn.

weight function evaluated at the ith quadrature point.

For the case of Gauss-Chebyschev quadrature this can be checked analytically: For Chebyschev quadrature of thr first kind we have[16]

$$\int_{-1}^{1} \frac{f(x)\,dx}{(1-x^2)^{1/2}} \cong \frac{\pi}{N} \sum_{n=1}^{N} f(x_n)\,, \qquad \text{(A3a)}$$

where

$$x_n = -\cos[(2n-1)\pi/2N]\,, \qquad \text{(A3b)}$$

$$\rho(x) = [(1-x^2)^{1/2}]^{-1} \qquad \text{(A3c)}$$

and $\omega_n = \pi/N$, independent of n.

TABLE VII. f- and g-wave elastic e^+-H(1s) phase shifts computed by the moment T-matrix method, compared with the adiabatic Dalgarno-Lynn (DL) phase shifts (Ref. 6).

	f-wave phase shifts			g-wave phase shifts			
k (a.u.)	A[a]	B[b]	DL	A[c]	B[d]	C[e]	DL
0.1	...	...	0.00045	...	...	...	0.000020
0.2	...	...	0.00187	...	...	...	0.00083
0.3	0.0036	0.0037	0.00416	...	...	...	0.00186
0.4	0.0069	0.0070	0.00753	0.00289	0.00289	0.00266	0.00334
0.5	0.117	0.118	0.1196	0.00480	0.00466	0.00467	0.00532
0.6	0.0185	0.0188	0.0173	0.00738	0.00733	0.07313	0.00778
0.7	0.0291	0.0286	0.0234	0.0109	0.0111	0.0109	0.01073

[a] 76-term basis $\alpha = 1.0$, $\beta = 0.7$.
[b] 76-term basis $\alpha = 1.0$, $\beta = 0.6$.
[c] 87-term basis $\alpha = 1.0$, $\beta = 0.6$.
[d] 87-term basis $\alpha = 1.0$, $\beta = 0.7$.
[e] 87-term basis $\alpha = 1.0$, $\beta = 0.8$.

TABLE VIII. Comparison of e^+-H(1s) phase shifts as computed by the Dalgarno-Lynn (DL), method (Ref. 6), and by the asymptotic (long-range) Born approximation (B) justifying the use of the asymptotic Born approximation for calculation of the $L = 10$ through 100 partial wave amplitudes needed in the computation of the angular distributions (an * indicates that the series expansion for the Born approximation has not fully converged).

	$L=0$		$L=2$		$L=8$		$L=10$	
k (a.u.)	DL	B	DL	B	DL	B	DL	B
0.1	0.181	−0.0476	0.00136	0.00132	2.92(−5)	2.92(−5)	1.55(−5)	1.54(−5)
0.2	0.241	−0.194	0.00555	0.00502	1.16(−4)	1.16(−4)	6.13(−5)	6.15(−5)
0.3	0.230	−0.433	0.0127	0.0102	2.62(−4)	2.61(−4)	1.38(−4)	1.38(−4)
0.4	0.191	−0.721	0.0225	0.0150*	4.68(−4)	4.63(−4)	2.46(−4)	2.45(−4)
0.5	0.141	−0.979*	0.0340	0.0165*	7.33(−4)	7.20(−4)	3.85(−4)	3.82(−4)
0.6	0.0893	−1.170*	0.0462	0.00983*	1.06(−3)	1.03(−3)	5.56(−4)	5.48(−4)
0.7	0.0399	−1.30*	0.0578	−0.0124*	1.45(−3)	1.39(−3)	7.59(−4)	7.42(−4)

Equation (A2) may be checked directly:

$$\frac{d}{d\xi}\left(-\cos[(2\xi-1)\pi/N]\right)\Big|_{\xi=n} = (1-x_n^2)^{1/2}\pi/N$$

which, indeed, is $\omega_n/\rho(x_n)$. A similar result holds for Chebyschev quadrature of the second kind (see Sec. V B of Yamani and Reinhardt, Ref. 16).

For the more general case the zeros of the required orthogonal polynomial are not known as analytic functions of i, yet the result holds empirically, as may be easily verified by interpolation of the numerically determined zeros. Using asymptotic representations (Szego[31]) of the classical orthogonal polynomials, Broad[17] has found that an analog of the Chebyschev result in the

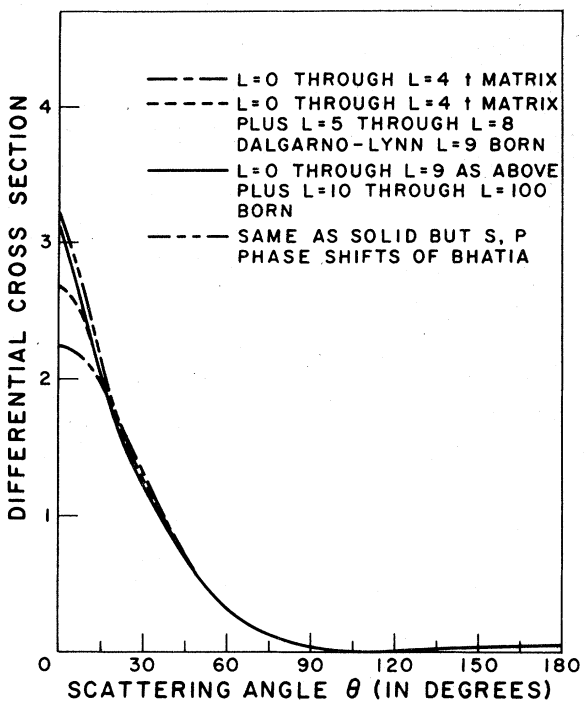

FIG. 9. Differential e^+-H(1s) elastic cross section (a_0^2/sr) at a positron energy $E = 0.08$ Hartrees (2.2 eV). Results are shown in several approximations: — - — in the cross section determined by the $L = 0 \rightarrow 4$ amplitudes of Tables IV–VII; - - - - shows the result of addition of the $L = 5 \rightarrow 8$ Dalgarno-Lynn adiabatic results and results and the $L = 9$ Born result; —— shows the result of supplementing these results with the $L = 10 \rightarrow 100$ Born amplitudes needed to achieve convergence in the forward direction. The — - — curve shows the 100 partial wave result with the more accurate Bhatia s and p-wave phase shifts: as discussed in the text the moment T-matrix method suffers at very low energies.

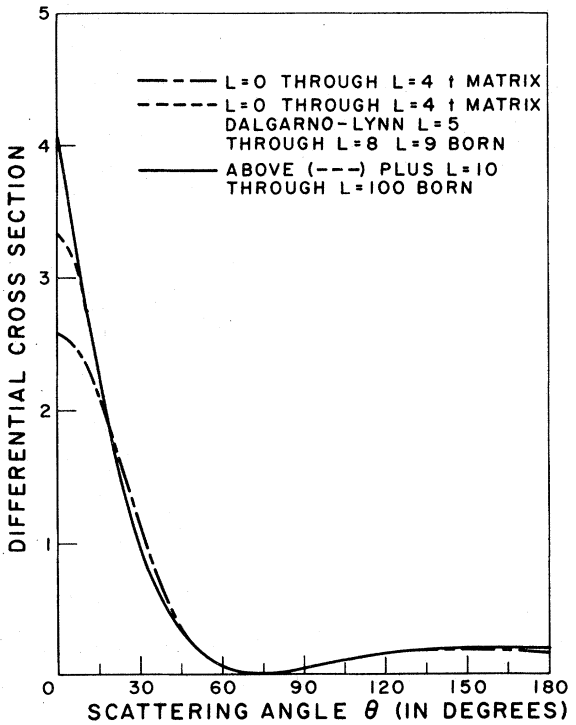

FIG. 10. Differential e^+-H(1s) elastic cross section (a_0^2/sr) at a positron energy of 0.18 Hartrees (4.9 eV) showing convergence as a function of the number of partial waves.

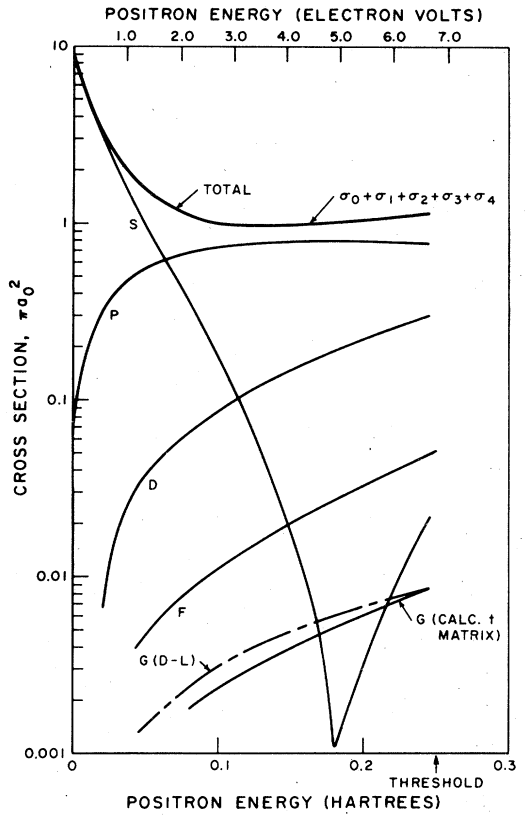

FIG. 11. Elastic integrated e^+-H cross section as a function of positron energy below the pick-up threshold. The total cross section and partial-wave contributions are shown. Convergence to better than 1% is obtained using the first five partial waves. As the g-wave and DL result gives a reasonable approximation to the T-matrix g-wave partial cross section, estimates of the magnitude of the contribution of higher partial waves was made by summing the $L=5\rightarrow 10$ Dalgarno-Lynn (DL) results and were at most 0.5%.

fact does hold, asymptotically, in the general case.

APPENDIX B: INTEGRAL EVALUATION

In this Appendix, we outline techniques for evaluation of integrals needed to construct $T_k(z)$ from $(z-\bar{H})^{-1}$.

A. Calculation of the Born term: the $\langle k|V|k\rangle$ integrals

The Born term integral may be easily reduced to the one-dimensional static integral

$$I_B=\int_0^\infty r^2[j_l(kr)]^2 e^{-2r}(1+1/r)\,dr\,. \tag{B1}$$

The integral

$$\int_0^\infty e^{-at}J_\nu(bt)J_\nu(ct)\,dt=\frac{1}{\pi\sqrt{bc}}\,Q_{\nu-1/2}\left(\frac{a+b+c}{2bc}\right) \tag{B2}$$

appears in Watson's treatise.[32] Since

$$j_l(kr)=(\pi/2kr)^{1/2}J_{l+1/2}(kr)\,, \tag{B3}$$

we have

$$\int_0^\infty re^{-2r}[j_l(kr)]^2\,dr=\frac{\pi}{2k}\int_0^\infty e^{-2r}(J_{l+1/2})^2\,dr$$
$$=\frac{1}{2k^2}\,Q_l\left(\frac{\alpha^2+2k^2}{2k^2}\right)_{\alpha=2} \tag{B4}$$

and, additionally

$$\int_0^\infty e^{-\alpha r}r^2[j_l(kr)]^2\,dr$$
$$=-\left[\frac{d}{d\alpha}\,\frac{1}{2k^2}\,Q_l\left(\frac{\alpha^2+2k^2}{2k^2}\right)\right]_{\alpha=2}, \tag{B5}$$

where the Q_l are the Legendre polynomials of the second kind.[33]

B. The $\langle k|V|\phi_i\rangle$ integrals

Since the potential $V=1/r_2-1/r_{12}$ does not operate on the angular functions, the angular integrations follow from Ref. 24, resulting in linear combinations of integrals of the form

$$\int_0^\infty r_1\,dr_1\int_0^\infty r_2\,dr_2\,e^{-(1+\alpha)r_1}e^{-\beta r_2}r_1^a r_2^b j_l(kr_2)$$
$$\times\int_{|r_1-r_2|}^{r_1+r_2} r_{12}^{c+1}\,dr_{12}\,. \tag{B6}$$

The integral over r_{12} yields

$$\frac{1}{c+2}\,r_{12}^{c+2}\Big|_{|r_1-r_2|}^{r_1+r_2}\,. \tag{B7}$$

The lower limit necessitates consideration of two cases: (a) $r_1>r_2$ for which $|r_1-r_2|=r_1-r_2$; (b) $r_2>r_1$ for which $|r_1-r_2|=r_2-r_1$. We get from case (a)

$$\frac{1}{c+2}\int_{r_2}^\infty e^{-(1+\alpha)r_1}r_1^{a+1}\,dr_1$$
$$\times\int_0^\infty e^{-\beta r_2}j_l(kr_2)\,r_2^{b+1}\,dr_2$$
$$\times[(r_1+r_2)^{c+2}-(r_1-r_2)^{c+2}]\,. \tag{B8a}$$

and from case (b)

$$\int_0^{r_2} e^{-(1+\alpha)r_1}r_1^{a+1}\,dr_1\int_0^\infty e^{-\beta r_2}\,j_l(kr_2)r_2^{b+1}\,dr_2$$
$$\times[(r_1+r_2)^{c+2}-(r_2-r_1)^{c+2}]\,. \tag{B8b}$$

Expanding the polynomials such as $(r_1+r_2)^n$ in binomial expansions, for case (a), we have

$$2\sum_{i=0}^{[(c+1)/2]}\binom{c+2}{2i+1}r_1^{c+1-2i}r_2^{2i+1} \tag{B9a}$$

where $[(c+1)/2]$ is the greatest integer in $(c+1)/2$: case (b) yields

$$2\sum_{i=0}^{[(c+1)/2]}\binom{c+2}{2i+1}r_2^{c+1-2i}r_1^{2i+1}\,. \tag{B9b}$$

Substituting into Eq. (B.7) we are left with: for case (a)

$$\frac{2}{c+2}\sum_{i=0}^{[(c+1)/2]}\binom{c+2}{2i+1}\int_0^\infty e^{-\beta r_2}j_l(kr_2)r_2^{p'}\,dr_2 \times\int_{r_2}^\infty e^{-(1+\alpha)r_1}r_1^{q'}\,dr_1\,, \tag{B10a}$$

and for case (b)

$$\frac{2}{c+2}\sum_{i=0}^{[(c+1)/2]}\binom{c+2}{2i+1}\int_0^\infty e^{-\beta r_2}j_l(kr_2)r_2^{q}\,dr_2 \times\int_0^{r_2} e^{-(1+\alpha)r_1}r_1^{p}\,dr_1\,, \tag{B10b}$$

where

$$p=a+2i+2\,,\quad q=b+c+2-2i\,,$$
$$p'=b+2i+2\,,\quad q'=a+c+2-2i\,.$$

Now the integrals over r_1 are performed yielding

$$\text{case (a)}=2\sum_{i=0}^{[(c+1)/2]}\binom{c+2}{2i+1} \times\int_0^\infty e^{-\beta r_2}j_l(kr_2)r_2^{p'}\,dr_2 \times\left(e^{-(1+\alpha)r_2}\sum_{j=0}^{q'}\frac{(q')!}{j!}\,\frac{r_2^j}{(1+\alpha)^{q'-j+1}}\right); \tag{B11a}$$

$$\text{case (b)}=2\sum_{i=0}^{[(c+1)/2]}\binom{c+2}{2i+1} \times\int_0^\infty e^{-\beta r_2}j_l(kr_2)r_2^{q}\,dr_2 \times\left(\frac{p!}{(1+\alpha)^{p+1}} - e^{(1+\alpha)r_2}\sum_{j=0}^{p}\frac{p'!}{j'}\,\frac{r_2^j}{(1+\alpha)^{p-j+1}}\right). \tag{B11b}$$

Thus we are left with double sums over integrals of the form

$$I=\int_0^\infty e^{-\gamma r}j_l(kr)r^n\,dr = \frac{\frac{1}{2}(k/2)^l\,\Gamma(n+l+1)\pi^{1/2}}{(\gamma^2+k^2)^{(l+n+1)/2}\Gamma(l+\frac{3}{2})} \times{}_2F_1\left(\frac{n+l+1}{2}\,,\ \frac{l-n+1}{2}\,,\ l+\tfrac{3}{2}\,;\ \frac{k^2}{k^2+\gamma^2}\right) \tag{B12}$$

which are conveniently calculated via the Gauss continued-fraction representations of ${}_2F_1(n,b;c;z)$, which form may be always obtained via a suitable Kummer transform.[33]

---

*Work completed while on leave from Dept. of Chemistry, Harvard University, Cambridge, Mass. 02138. Present address: Laboratory for Atmospheric and Space Physics, University of Colorado, Boulder, Colo. 80309.

[1]H. S. W. Massey and C. B. O. Mohr, Proc. Phys. Soc. Lond. 67, 695 (1954).

[2]J. R. Winick and W. P. Reinhardt, Phys. Rev. A 18, 925 (1978) (following paper).

[3]J. R. Winick, Ph.D. thesis (Harvard University, 1976) (unpublished).

[4]A. K. Bhatia, A. Temkin, R. J. Drachman, and H. Eiserike, Phys. Rev. A 3. 1328 (1971); A. K. Bhatia, A. Temkin, and H. Eiserike, *ibid.* 9, 219 (1974).

[5]For example, see R. P. McEachran and P. A. Fraser, Proc. Phys. Soc. Lond. 86, 369 (1965).

[6]R. J. Drachman, Phys. Rev. 138, A 1582 (1965); A. Dalgarno and H. Lynn, Proc. Phys. Soc. Lond. A 70, 223 (1957); R. J. Drachman and A. Temkin, in *Case Studies in Atomic Collision Physics II*, edited by E. W. McDaniel and M. R. C. McDowell (North-Holland, Amsterdam, 1972), p. 401.

[7]C. Schwartz, Phys. Rev. 124, 1468 (1961); R. L. Armstead, *ibid.* 171, 91 (1968); D. Register and R. J. Poe, Phys. Lett. A 51, 431 (1975).

[8]L. Schlessinger and C. Schwartz, Phys. Rev. Lett. 16, 1173 (1966); L. Schlessinger, Phys. Rev. 171, 1523 (1968).

[9]T. N. Rescigno and W. P. Reinhardt, Phys. Rev. A 10, 158 (1974).

[10]G. Doolen, G. McCartor, F. A. McDonald, and J. Nuttall, Phys. Rev. A 4, 108 (1971).

[11]E. Gerjuoy, in *The Physics of Electronic and Atomic Collisions*, VII ICPEAC Invited Papers and Progress Reports, edited by T. R. Govers and F. J. deHeer (North-Holland, Amsterdam, 1972), p. 247; F. W. Byron, Jr., in *Atomic Physics*, edited by G. zu Putlitz, E. W. Weber, and Q. Winnacker (Plenum, New York, 1975), Vol. IV, p. 337; B. H. Bransden and

M. R. C. McDowell, Phys. Rep. 30, 208 (1977).
[12]For example, see N. F. Mott and H. S. W. Massey, *The Theory of Atomic Collisions*, 3rd ed. (Oxford U. P., Oxford, 1965); K. C. Bell, and A. E. Kingston, Adv. At. Mol. Phys. 10, 53 (1974).
[13]E. W. Montroll, J. Chem. Phys. 10, 218 (1942); 11, (1943); J. Deltour, Physica (Utr.) 39, 413, 424, 431 (1968).
[14]P. W. Langhoff, Chem. Phys. Lett. 22, 60 (1973); P. W. Langhoff, and C. T. Corcoran, J. Chem. Phys. 61, 146 (1974); P. W. Langhoff, J. Sims, and C. T. Corcoran, Phys. Rev. A 10, 829 (1974).
[15]R. J. Drachman, in *The Physics of Electronic and Atomic Collisions*, VII ICPEAC Invited Papers and Progress Reports, edited by T. R. Grovers and F. J. de-Heer (North-Holland, Amsterdam, 1972), p. 277; B. H. Bransden, in *Case Studies in Atomic Collison Physics I*, edited by E. W. McDaniel and M. R. C. McDowell (North-Holland, Amsterdam, 1969), p. 171.
[16]E. J. Heller, Ph.D. thesis (Harvard University) (unpublished). A discussion appears in H. A. Yamani and W. P. Reinhardt, Phys. Rev. A 11, 1144 (1975). See also Appendix A.
[17]J. T. Broad (private communication).
[18]R. G. Newton, *Scattering Theory of Waves and Particles* (McGraw-Hill, New York, 1966), p. 186 *et seq.* J. R. Taylor, *Scattering Theory* (Wiley, New York, 1972), p. 42 *et seq.*
[19]For examples of recent work on the analysis of the e^-–H amplitude see A. Tip, J. Phys. B 10, L295 (1977), and references therein.
[20]F. A. McDonald and J. Nuttall, Phys. Rev. Lett. 23, 361 (1969).
[21]W. P. Reinhardt, Phys. Rev. A 8, 754 (1973).
[22]E. J. Heller, W. P. Reinhardt, and H. A. Yamani, J. Comput. Phys. 13, 536 (1973); H. A. Yamani and W. P. Reinhardt, Ref. 16.
[23]E. J. Heller and W. P. Reinhardt, Phys. Rev. A 7, 365 (1973); E. J. Heller, T. N. Rescigno, and W. P. Reinhardt, *ibid.* 8, 2946 (1973).
[24]J. L. Calais and P. O. Lowdin, J. Mol. Spectrosc. 8, 203 (1962).
[25]C. Schwartz, Phys. Rev. 123, 1700 (1961).
[26]T. S. Murtaugh and W. P. Reinhardt, J. Chem. Phys. 57, 129 (1972).
[27]J. H. Wilkinson, *The Algebraic Eigenvalence Problem* (Oxford U. P., Oxford, 1965), p. 282 *et seq.*
[28]C. B. Moler and G. W. Stewart, Stanford University Report STAN CS-232-71, 1971 (unpublished). Routine available through the International Mathematical and Statistical Library (IMSL), Inc., program library.
[29]R. A. Sack and A. E. Donovan, Numer. Math. 18, 465 (1972).
[30]J. Calloway and J. F. Williams, Phys. Rev. A 12, 2312 (1975).
[31]G. Szego, *Orthogonal Polynomials* (American Mathematical Society, Providence, Rhode Island, 1967), 3rd ed., Chap. 8.
[32]G. N. Watson, *Treatise on the Theory of Bessel Functions* (Cambridge U. P., Cambridge, 1966), 2nd ed., p. 389.
[33]M. A. Abramowitz and I. A. Stegun, *Handbook of Mathematical Functions*, NBS Appl. Math Ser. 55, p. 331.